Pergamon

SCIENCE DIRECT®

Tetrahedron 59 (2003) 2409–2415

TETRAHEDRON

Calixarene-based metalloporphyrins: molecular tweezers for complexation of DABCO

Miroslav Dudič,[a] Pavel Lhoták,[a,*] Hana Petříčková,[b] Ivan Stibor,[a] Kamil Lang[c,*] and Jan Sýkora[d]

[a]*Department of Organic Chemistry, Prague Institute of Chemical Technology, Technická 5, 166 28 Prague 6, Czech Republic*
[b]*Department of Solid State Chemistry, Institute of Chemical Technology, Technická 5, 166 28 Prague 6, Czech Republic*
[c]*Institute of Inorganic Chemistry, ASCR, 250 68 Řež, Czech Republic*
[d]*Institute of Chemical Process Fundamentals, ASCR, Rozvojova 135, 165 02 Prague 6, Czech Republic*

Received 2 December 2002; revised 24 January 2003; accepted 21 February 2003

Abstract—We investigated the formation of host–guest complexes between zinc porphyrins covalently attached to calixarenes via amidic bonds and a small bidentate ligand bearing two nitrogen atoms. Depending upon the calixarene structure (S vs CH_2 bridges), the ligand 1,4-diazabicyclo[2.2.2]octane (DABCO) is complexed by metalloporphyrin units by two different ways. While the thiacalix[4]arene prefers an intramolecularly closed cavity with a binding constant of $(1.0\pm0.1)\times10^7\ M^{-1}$ in $CHCl_3$ at 294 K (stoichiometry 1:1), the classical calix[4]arene forms a complex by ligation of both porphyrin units separately (stoichiometry 2:1). The differences observed can be rationalized in terms of cavity size and the preorganization due to intramolecular hydrogen bonding of the calixarene lower rim.

1. Introduction

Many porphyrin oligomers have been studied in order to better understand host–guest interactions, molecular recognition phenomena and photoinduced processes related to natural photosynthetic systems and enzyme mimics.[1] Ligand selectivity and recognition are driven by simultaneous cooperation of various non-covalent interactions between porphyrin structures and covalent bonding of axial ligands to a metal center. Zinc porphyrins are known to bind an axial ligand to form five-coordinated complexes that have been studied as components for molecular devices, conjugated porphyrin polymers, supramolecular systems and light harvesting models.[2]

On the other hand, calixarenes represent a well-known family of macrocyclic compounds[3] with many unique properties. The three-dimensional shape of these molecules is directed by their conformation and can be readily controlled. This makes calixarenes extremely useful in supramolecular chemistry[4] as building blocks and/or molecular scaffolds. In this paper we report on the synthesis of zinc porphyrins bound to the (thia)calixarene skeleton by an amidic spacer. The spacer gives the compound flexibility for adjusting the distance between the porphyrin units. The formation of a closed cavity is based on metal-to-ligand interactions of two porphyrin units with a bidentate ligand.

2. Results and discussion

2.1. Synthesis

As the macrocyclic scaffold, we have chosen calix[4]arene **1** and thiacalix[4]arene **2**, which are easily accessible in a multigram scale.[5] These compounds were transformed into the corresponding diacetates and tetraacetates using ethyl bromoacetate/K_2CO_3 in refluxing acetone. Hydrolysis with NaOH in aqueous ethanol under reflux yielded the corresponding carboxylic acids. (Thia)calix[4]arene diamides **3** and **4** were prepared directly from diacids using monoamino derivative of 5,10,15,20-tetraphenylporphyrin (MAP)[6] in the presence of DCC (78 and 72% yields, respectively), while tetraamides **5** and **6** were prepared via the corresponding acyl chlorides in 45 and 71% yields, respectively (Scheme 1).[6] The metallation of porphyrins was achieved using zinc acetate/Et_3N in anhydrous CH_2Cl_2 to yield the corresponding products **7** (96%), **8** (96%), **9** (85%) and **10** (70%). The *cone* conformations of novel metalloporphyrin derivatives were proven using ^1H and ^{13}C NMR spectroscopy. Thus, the ^1H NMR spectrum of thiacalixarene **8** consists of two sets of Bu^t (δ=1.25 and 1.36 ppm) that reflects a C_{2v} symmetry typical for a diametrically substituted *cone* conformer. Similarly,

Keywords: porphyrins; calixarenes; DABCO.

* Corresponding authors. Tel.: +420-2-2435-5048; fax: +420-2-2435-4288; lhotakp@vscht.cz; lang@iic.cas.cz

0040–4020/03/$ - see front matter
doi:10.1016/S0040-4020(03)00290-4

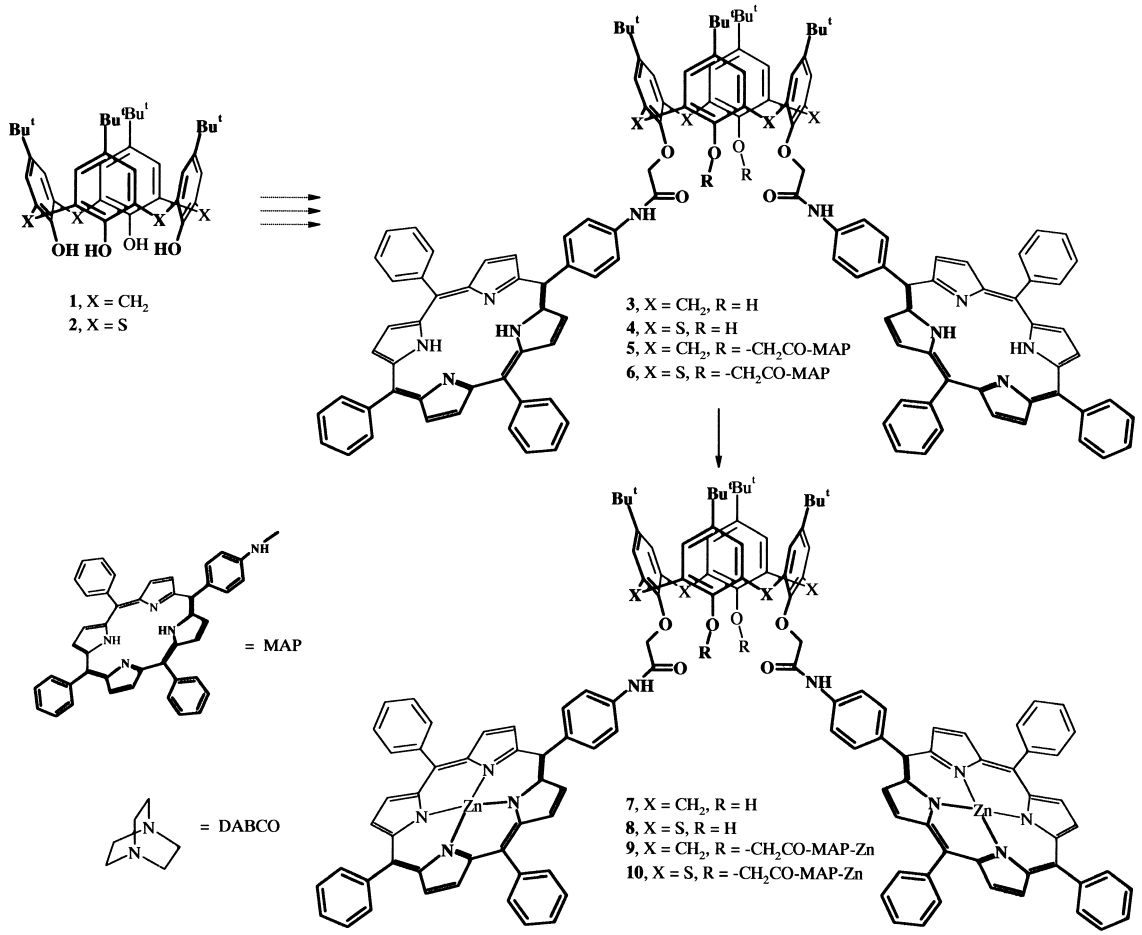

Scheme 1. (i) $Zn(OAc)_2/Et_3N$, CH_2Cl_2, room temperature (**3**→**7**, 96%; **4**→**8**, 96%; **5**→**9**, 85%; **6**→**10**, 70%).

tetrasubstituted compounds **9** and **10** exhibit a cone pattern with C_{4v} symmetry.

2.2. Spectroscopic properties

Electronic absorption spectra of **8** and **10** show maxima at 550 and 588 nm for the Q(1,0) and Q(0,0) bands that are similar to ZnTPP[7] (548, 586 nm). In contrast, the Soret bands are considerably broadened and split into doublets as evidenced by the corresponding second derivative. The doublets are separated by 8 nm (12 nm in $CHCl_3$, Figure 1) and 7 nm (14 nm in $CHCl_3$) for **8** and **10** in CH_2Cl_2, respectively. This indicates intramolecular exciton coupling between closely separated porphyrin units in the excited S_2 states. Similar features were also observed in spectra of free-base calixarene–porphyrins,[6] covalently linked porphyrin dimers[8] and porphyrin arrays.[9,10] According to a point-dipole approximation of the exciton coupling model a spectral red-shift is attributed to a head-to-tail dimer and a blue-shifted band is due to a face-to-face dimer.[11] The band splitting observed in our spectra is typical for an oblique geometry where the respective intensities of the split Soret bands reflect the orientation of the porphyrin units relative to each other. The same spectral properties were also observed for the methylene bridged calixarenes **7** and **9**. The correspondence of the bands in the Q region with those observed for monomer ZnTPP is due to the fact that transition moments involved between the S_1 states are much smaller than those between the S_2 states. We corroborated this by observing that the fluorescence quantum yield of dimers **8** (Φ_f=0.043) and **7** (Φ_f=0.042) are similar to that of ZnTPP[7] (Φ_f=0.03). Porphyrin tetramers **9** (Φ_f=0.033) and **10** (Φ_f=0.035) have slightly reduced Φ_f compared to **7** and **8**, respectively, due to more effective exciton coupling

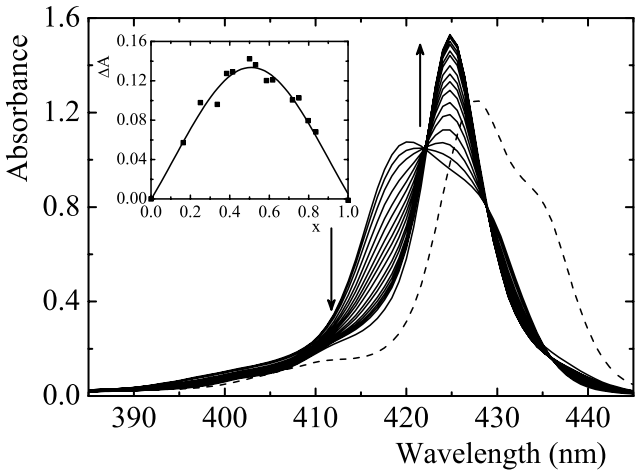

Figure 1. UV/Vis titration of 1.5 μM **8** with DABCO in CH_3Cl. The arrow shows increasing concentration of DABCO. The dotted line represents the complex $(DABCO)_2$–**8**. Inset: Job plot for binding DABCO to **8** recorded at 418 nm. The sum of the total concentrations of interacting components is constant (1.3 μM), x is the mole fraction of DABCO.

within four porphyrin units located on the lower rim of the calixarene regardless of the calixarene bridging group. The observed spectral splitting is solvent dependent due to the spatial flexibility of the spacer connecting the porphyrin units and calixarene. In general, more polar solvents such as methanol induce stronger exciton coupling.[6]

2.3. Complexation study

With the addition of 1,4-diazabicyclo[2.2.2]octane (DABCO) the original split Soret band of **8** sharpens and is red-shifted (Fig. 1) as a consequence of the ligand-**8** complexation. The features of the new Soret band are also observed upon addition of axial ligands to ZnTPP and clearly differentiate axially ligated ZnTPP from free ZnTPP.[7] Titration with DABCO in $CHCl_3$ results in well-defined isosbestic points at 422, 429 and 436 nm (Fig. 1) and in a sharp saturation beyond the concentration ratio DABCO/**8** of 1:1 (Fig. 2(a)). These findings together with the maximum at the mole fraction of 0.5 on the Job plot (Fig. 1, inset) confirm the presence of two absorbing species in equilibrium and the formation of a 1:1 host–guest complex. Analysis of titration data by a non-linear least-squares fitting procedure provided the binding constant of $(1.0\pm0.1)\times10^7\ M^{-1}$ in $CHCl_3$ at 294 K. The disappearance of the split Soret band is due to the formation of an intramolecular cofacial porphyrin dimer in which both zinc ions are ligated to the opposite nitrogens of DABCO. Binding of bidentate DABCO separates the porphyrin units, increases their mutual distance and locks their mutual orientation. All these factors eliminate exciton splitting. This way DABCO forms a lid for the cavity consisting of the lower calixarene rim and two connected porphyrin units. The binding stoichiometry of 1:1 was also confirmed by ^1H NMR (300 MHz) using the Job plot procedure. The binding constant is much higher than that observed for monomeric Zn–porphyrin (e.g. $2.4\times10^5\ M^{-1}$)[12] showing that DABCO is bound extremely strongly within the cavity due to a cooperate effect of both metalloporphyrin subunits. The complex is stable and is the dominant species in mixtures of DABCO/**8** at molar concentration ratios up to 250:1. A larger excess of DABCO (molar ratio ≈6000:1) is needed to destabilize the 1:1 complex. Under these conditions a new complex $(DABCO)_2$–**8** is formed having the split Soret band separated by 9 nm (Fig. 1) as a result of exciton coupling between both porphyrin units each bearing one bound DABCO molecule. Surprisingly, the Soret band of **7** is shifted similarly to **8**, but remains broad and split (Fig. 3). The binding isotherm exhibits a clearly sigmoidal profile with saturation at higher excess of DABCO, indicating unambiguously the cooperative nature of the complexation between DABCO and **7** (Fig. 3, inset). The formation of the 1:1 complex is never complete. In contrast to **8**, the isosbestic point gradually shifts during titration leading to the final split Soret band indicating that the preferred structure of **7** is the complex $(DABCO)_2$–**7** with one ligand *per* porphyrin unit. It is evident that **7** and **8** slightly differ in size and that the amidic spacer compensates for these small differences because the ligand bond is distant from the calixarene skeleton. Our finding shows that binding of DABCO is very sensitive to subtle changes in the structure mediated by the calixarene CH_2/S bridges. Binding of DABCO by porphyrin tetramers **9** or **10** is more complex because four potential binding sites are available. In these cases, the addition of DABCO is followed by a sharpening and by a red shift of the Soret band. The Job plots confirm the formation of a 1:1 complex in the first step, the sigmoidal curvatures on the binding isotherms (Fig. 2(b)), however, documents that the complexation is hindered by stacking of the porphyrin units within the molecule.

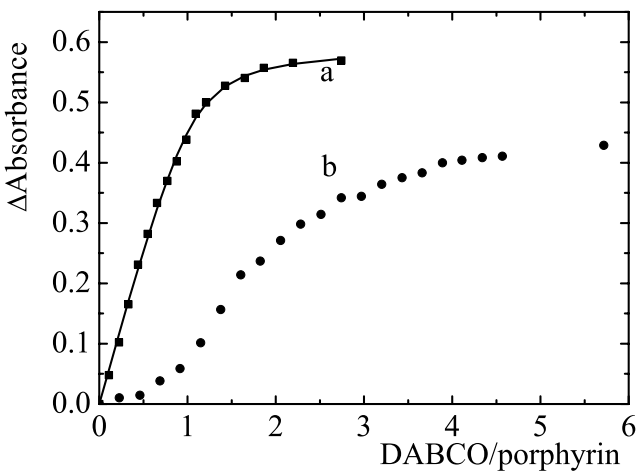

Figure 2. The binding isotherms of 1.5 μM **8** (a) and 1.1 μM **10** (b) at 425 and 426 nm in $CHCl_3$, respectively. The solid line is the theoretical isotherm for the complex DABCO-**8** obtained by least squares fit to the experimental data using the hyperbolic equation.

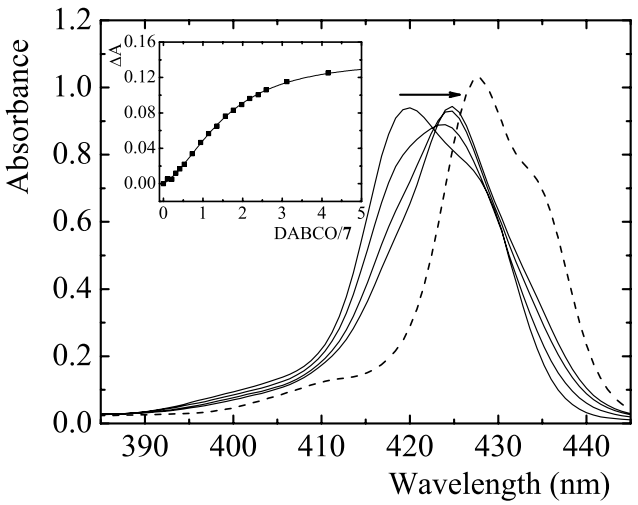

Figure 3. UV/Vis titration of 1.3 μM **7** with DABCO in CH_3Cl. The arrow shows a shift of the isosbestic point during titration. From left: **7** in the absence and in the presence of 1.7, 4.0 and 6.7 μM DABCO. The dotted line represents the complex $(DABCO)_2$–**7**. Inset: the binding isotherm at 425 nm.

2.4. Structural study

As we have shown previously[13–15] the thiacalix[4]arene cavity is larger than that of CH_2-bridged calixarene. The distances between two neighboring and between two opposite sulphur atoms in the *cone* thiacalixarene tetra-acetate {5,11,17,23-tetra-*tert*-butyl-25,26,27,28-tetra-kis[(ethoxy-carbonyl)methoxy]-2,8,14,20-tatrathiacalix(4)-arene} are 5.48 and 7.67 Å, respectively, while the typical distances between the CH_2 groups in the corresponding classical analog are 5.11 and 7.16 Å.[13] In accordance with

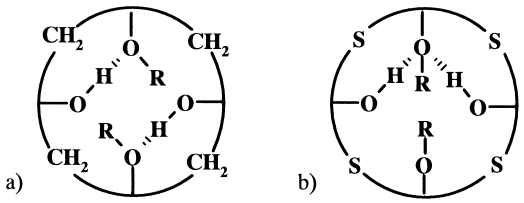

Figure 4. Arrangement of hydrogen bonds in distally disubstituted: (a) calix[4]arene and (b) thiacalix[4]arene derivatives (schematically).

this, substantially different conformational behavior of thiacalixarene derivatives was found both in solution[15] and in the solid[14] state. An illustrative example of different chemical reactivity, originating from the different cavity size, is the formation of intramolecular lactones in the thiacalixarene series—a reaction never observed in classical calix[4]arene chemistry.[16]

The complexation study indicated the quite diverse behaviour of thiacalixarene diamide **8** when compared with the corresponding calix[4]arene **7**. A plausible explanation of this phenomenon could be ascribed to differences in the cavity size. The larger cavity of thiacalixarene **8** better fits steric requirements of DABCO, which results in the formation of the intramolecular 1:1 complex. On the other hand, the smaller cavity of **7** tends to prefer the 2:1 complex.

The ^{1}H NMR study of **7** and **8** did not indicate any differences in the conformational behavior of both compounds. Unfortunately, our attempts to grow suitable monocrystals for X-ray study have also failed. Hence, we have turned our attention to simplified model structures to show different behavior and/or preferences of thiacalixarenes. As model compounds we used corresponding diacetates **11**–**14** that are intermediates during the synthesis of diamides **7** and **8**.

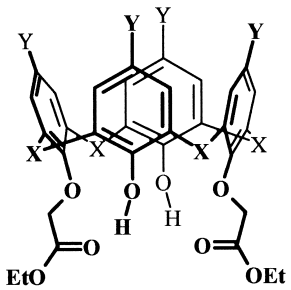

11, X = CH_2, Y = H
12, X = CH_2, Y = Bu^t
13, X = S, Y = H
14, X = S, Y = Bu^t

To our surprise, the crystallographic study revealed an uncommon hydrogen bonding pattern. It is well known,[3] that distally disubstituted classical calix[4]arene derivatives adopt the *cone* conformation held together by the circular hydrogen bond array. The free OH groups on the lower rim of calixarene interact with both neighbor substituents in a manner schematically depicted in Figure 4(a). This arrangement, also found in the solid-state structure of **11**, leads to molecules with approximately C_2 symmetry. On the contrary, thiacalixarenes **13** and **14** were proven to adopt very unusual structures where both free opposite hydroxyls interact with the same OR group causing a lower overall symmetry (Fig. 4(b)).

Thus, compound **11**[17] adopts the *cone* conformation with two almost symmetrically situated hydrogen bonds[18] (Fig. 5(a)). The H1···O15 and H4···O1 distances are 1.92 and 2.06 Å, respectively, with corresponding O7–H1–O15 and O26–H4–O1 angles being approx. 165°. This arrangement leads to the cavity having almost C_4 symmetry (considering only phenolic units). Both substituents on the lower rim are oriented out from the cavity (Fig. 6(a)) with the distance between ester oxygens being 7.10 Å.

On the other hand, thiacalixarene diacetates **13**[19] and **14**[20] prefer other conformation, virtually unknown in classical calix[4]arene chemistry. Figure 5(b) shows the structure of compound **13**, where both OH groups are hydrogen bonded with the same oxygen atom O6 (distances O6···O7=2.98 Å and O6···O9=2.94 Å, compare with O5···O7=3.80 Å and O5···O9=3.92 Å). An almost identical conformation was also found in the case of diester **14** (Fig. 5(c)). The corresponding O···O distances (O1···O4=2.90 Å, O3···O4=3.08 Å vs O1···O2=O3···O2=3.84 Å) again clearly indicate asymmetrical arrangement of hydrogen bonds. As a consequence, the molecule possesses lower symmetry with two opposite phenolic units being symmetrically tilted (with the upper rims) out of the cavity. The third aromatic subunit is almost perpendicular to the main plane of the molecule formed by the four sulphur atoms, while the opposite fourth phenolic unit is inclined towards this subunit by its upper rim (Fig. 6(b)). The unsymmetrical organization of the upper rim results in changes to the lower rim arrangement. Accordingly, the distance between two ester oxygen atoms is 4.66 Å, which is much shorter (cf. 7.10 Å) than in the corresponding classical calix[4]arene **11**.

The above-described conformation differences of both

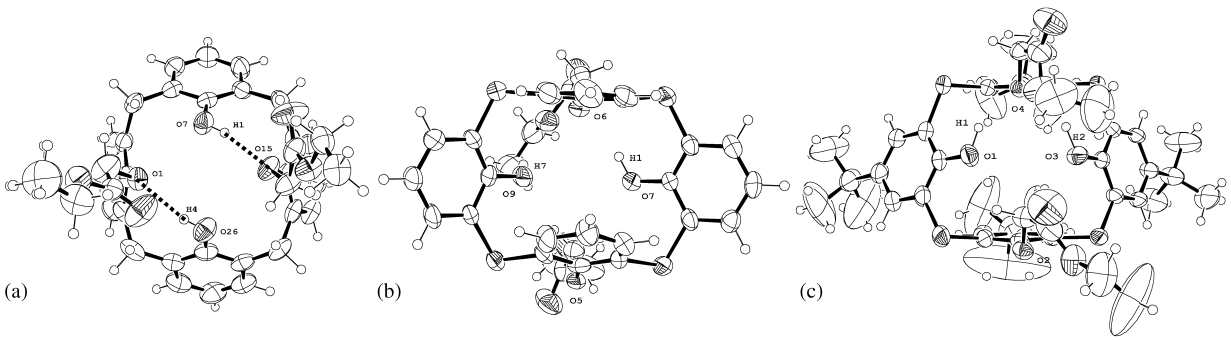

Figure 5. ORTEP drawing of derivatives **11**, **13** and **14**.

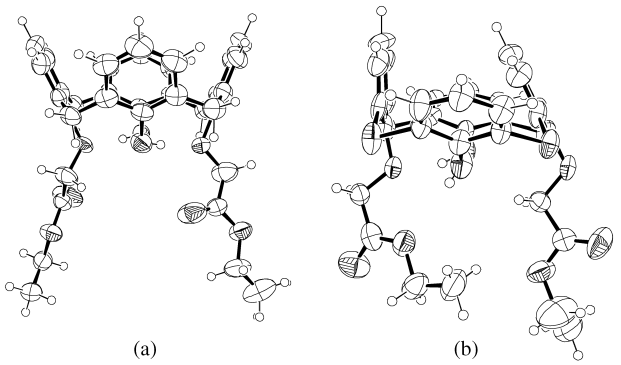

Figure 6. ORTEP drawing of derivatives **11** and **13**.

classical calixarenes and thiacalixarenes could be used as fundamentals for the explanation of different complexation ability towards DABCO. Although we were unable to prove the same type of hydrogen bonding pattern experimentally in the solution, our crystallographic results are indicative of the specific behavior of both molecular systems.

2.5. Conclusions

It is worth noting that the interconnecting structural motif induced by DABCO has been reported for anthracene-bridged bisporphyrins,[23] covalent cofacial porphyrin dimers,[12] conjugated porphyrin.[10,24] We have shown that calixarene-based Zn^{2+}-metalloporphyrins, depending upon a (thia)calixarene structure, can also act as a host for the bidentate guests such as DABCO. The basically novel feature of our compounds is the fact that the mode and the stoichiometry (1:1 vs 1:2) of complexation strictly depend on the calixarene (thia vs classical) used as a scaffold in the design of receptors. Self-organization of metalloporphyrins to form closed assemblies opens new ways for the utilization of calixarenes for sensing other species, e.g. anions. Tuning the complexation ability of calixarene–porphyrin conjugates is currently underway in our laboratories.

3. Experimental

3.1. General

Melting points are uncorrected and were determined using a Boetius Block apparatus. ^{1}H NMR spectra were recorded on a Varian Gemini 300 and a Bruker AMX3 400 spectrometers using tetramethyl silane as an internal standard. FAB MS were measured on a ZAB-EQ VG Analytical spectrometer. Dichloromethane used for the synthesis was dried with CaH_2 and stored over molecular sieves. Elemental analyses of the calixarene–porphyrin conjugates **7**–**10** resulted in C values approx. 2% lower than the calculated values. This phenomenon is well known in the calixarene chemistry[25] and we believe that the structures of the calixarenes are sufficiently proved by the spectral evidences.

Compounds **3**,[6] **4**,[6] **5**,[6] **6**,[6] **11**,[26] **12**,[27] **13**,[28] and **14**[28] were prepared according to known procedures.

3.1.1. Synthesis of derivative 7. A solution of compound **3** (60 mg; 3.02×10^{-2} mmol), $(CH_3COO)_2Zn\cdot2H_2O$ (27 mg; 0.12 mmol) and Et_3N (catalytic amount) in absolute CH_2Cl_2 (5 ml) was stirred for 2 h. The solvent was then evaporated and the crude residue was purified by column chromatography on silica gel ($CHCl_3$–petroleum ether 4/1 with 2% Et_3N) to yield 63 mg of pure product **7** (96% yield, R_f=0.58 ($CHCl_3$–petroleum ether 4/1)) in the form of violet microcrystals. Mp >350°C ($CHCl_3$–EtOH). ^{1}H NMR (400 MHz, $CDCl_3$) δ 1.18 (s, 18H, Bu^t), 1.32 (s, 18H, Bu^t), 3.69 (d, 4H, J=13.1 Hz, Ar*CH*$_2$Ar), 4.89 (d, 4H, J=12.88 Hz, Ar*CH*$_2$-Ar), 4.92 (s, 4H, -*CH*$_2$CO–), 7.15 (s, 4H, H-arom), 7.23 (s, 4H, H-arom), 7.69 (m, 20H, H-arom), 8.16 (m, 10H, H-arom), 8.27 (m, 8H, H-arom), 8.84 (s, 2H, Ar*OH*), 8.88 (s, 8H, H-arom), 8.96 (d, 4H, J=4.57 Hz, H-arom), 9.27 (d, 4H, J=4.57 Hz, H-arom), 11.08 (s, 2H, H-arom). ^{13}C NMR (100 MHz, $CDCl_3$) δ 31.08, 31.63, 32.67, 34.05, 34.35, 75.11, 117.57, 120.89, 121.01, 126.01, 126.42, 126.69, 127.31, 127.37, 131.79, 132.17, 132.47, 132.57, 134.36, 134.92, 137.53, 139.11, 142.88, 142.94, 143.86, 148.57, 149.14, 149.53, 150.02, 158.11, 150.29 150.66, 165.90. IR ($CHCl_3$) ν_{max} (cm^{-1}): 1689 (C=O), 3319 (NH, OH). UV–Vis (CH_2Cl_2) λ_{max} (nm), ε ($M^{-1}cm^{-1}$) in parentheses: 417 (7.9×10^5), 549 (4.2×10^4), 586 (8.6×10^3). Fluorescence (CH_2Cl_2), λ_{max} (nm): 598, 646. FAB MS *m*/*z* (rel. int.) 2117 $[M+1]^+$ (100).

3.1.2. Synthesis of derivative 8. A mixture of diamide **4** (70 mg, 3.4×10^{-2} mmol), $(CH_3COO)_2Zn\cdot2H_2O$ (30 mg, 0.14 mmol) and Et_3N (catalytic amount) in anhydrous CH_2Cl_2 (5 ml) was stirred overnight at room temperature. The solvent was removed under reduced pressure and the crude product was purified by column chromatography on silica gel using a $CHCl_3$–petroleum ether (4:1) mixture with 1% Et_3N as an eluent to give the pure product **8** as dark violet crystals (70 mg, 96%, R_f=0.48 ($CHCl_3$–petroleum ether 4/1)). Mp >350°C ($CHCl_3$–MeOH). ^{1}H NMR (300 MHz, $CDCl_3$) δ 1.25 (s, 18H, Bu^t), 1.36 (s, 18H, Bu^t), 4.97 (s, 4H, *CH*$_2$CO), 7.68 (m, 8H, H-arom), 7.74 (s, 8H, H-arom), 7.84 (s, 4H, H-arom), 8.20 (m, 18H, H-arom), 8.30 (t, 4H, J=8.79 Hz, H-arom), 8.92 (s, 12H, H-arom), 9.01 (d, 4H, J=4.76 Hz, H-arom), 9.34 (d, 4H, J=4.76 Hz, H-arom), 9.39 (s, 2H, Ar*OH*), 11.03 (s, 2H, *NH*CO). ^{13}C NMR (100 MHz, $CDCl_3$): δ 30.98, 31.41, 34.28, 34.68, 76.29, 117.76, 120.65, 120.76, 120.94, 121.10, 126.38, 126.42, 127.25, 127.32, 128.18, 131.67, 131.73, 132.12, 132.61, 134.38, 134.97, 135.74, 136.81, 137.69, 138.90, 142.94, 143.01, 144.42, 149.96, 150.05, 150.29, 150.52, 150.74, 156.69, 157.21, 165.60. IR ($CHCl_3$) ν_{max} (cm^{-1}): 1690 (C=O), 3323 (OH, NH). UV–Vis (CH_2Cl_2) λ_{max} (nm), ε (M^{-1} cm^{-1}) in parentheses: 418 (8.0×10^5), 550 (4.2×10^4), 587 (8.6×10^3). Fluorescence (CH_2Cl_2), λ_{max} (nm): 598, 646. FAB MS *m*/*z* (rel. int.) 2189 $[M+1]^+$ (100).

3.1.3. Synthesis of derivative 9. Using similar procedure as described above for **7** (85% yield, R_f=0.64 ($CHCl_3$–AcOEt 15/1), violet crystals). Mp >350°C ($CHCl_3$–MeOH). ^{1}H NMR (300 MHz, $CDCl_3$) δ 1.22 (s, 36H, Bu^t), 3.56 (brs, 4H, Ar*CH*$_2$Ar), 4.79 (brs, 12H, Ar*CH*$_2$Ar and *CH*$_2$CO), 6.98 (brs, 24H, H-arom), 7.44 (brs, 16H, H-arom), 7.68 (brs, 28H, H-arom), 8.10 (brs, 24H, H-arom), 8.64 (m, 24H, H-arom), 9.63 (brs, 4H, CO*NH*). ^{13}C NMR (100 MHz, $CDCl_3$) δ 29.70, 31.49, 119.02, 120.67, 125.82, 126.42,

126.75, 127.30, 131.58, 133.91, 134.41, 135.28, 142.25, 142.86, 149.79. IR ($CHCl_3$) λ_{max} (cm^{-1}): 1681 (C═O), 3029 (NH). UV–Vis (CH_2Cl_2) λ_{max} (nm), ε ($M^{-1}\,cm^{-1}$) in parentheses: 420 (9.6×10^5), 549 (6.6×10^4), 588 (1.4×10^4). Fluorescence (CH_2Cl_2), λ_{max} (nm): 600, 648. FAB MS *m/z* (rel. int.) 3583 $[M+1]^+$ (100).

3.1.4. Synthesis of derivative 10. This procedure is similar to that described for **8**. The pure product was obtained as violet micro crystals (34 mg, 70%, R_f=0.81 ($CHCl_3$–AcOEt 25/1)). Mp >300°C ($CHCl_3$–MeOH). ^1H NMR (300 MHz, $CDCl_3$) δ 1.27 (s, 36H, Bu^t), 5.10 (brs, 8H, CH_2CO), 6.93 (brs, 16H, H-arom), 7.04 (brs, 8H, H-arom), 7.56 (brs, 24H, H-arom), 7.70 (brs, 16H, H-arom), 8.13 (m, 28H, H-arom), 8.60 (brs, 8H, H-arom), 8.72 (brs, 8H, H-arom), 8.76 (brs, 8H, H-arom), 10.04 (s, 4H, *NH*CO). ^{13}C NMR (100 MHz, $CDCl_3$): δ 31.24, 34.52, 75.62, 118.55, 120.37, 120.64, 125.84, 126.39, 126.72, 127.27, 127.95, 131.54, 131.69, 132.03, 133.99, 134.41, 135.23, 135.33, 136.98, 139.44, 142.45, 142.97, 148.12, 149.80, 149.88, 150.16, 158.04, 167.17. IR ($CHCl_3$) ν_{max} (cm^{-1}): 1688 (C═O), 3327 (NH). UV–Vis (CH_2Cl_2) λ_{max} (nm), ε ($M^{-1}\,cm^{-1}$) in parentheses: 420 (1.05×10^6), 549 (7.3×10^4), 588 (1.6×10^4). Fluorescence (CH_2Cl_2), λ_{max} (nm): 599, 648. FAB MS *m/z* (rel. int.) 3655 $[M+1]^+$ (100).

3.2. Complexation study

All titration experiments were repeated several times in $CHCl_3$ at 294 K. The binding isotherms were analyzed using the hyperbolic relationship between the observed absorbance change ($\Delta A=A-A_0$) and the equilibrium free molar concentration of the guest [L]:

$$\Delta A = \frac{\Delta A_\infty K_b[L]}{1 + K_b[L]},$$

where K_b is the binding constant, A_0 is the absorbance in the absence of the guest and $\Delta A_\infty=A_\infty-A_0$. The free molar concentration was expressed as a function of the added total guest concentration using $L_t=[L]+P_tK_b[L]/(1+K_b[L])$, where P_t is the total molar concentration of **8**.[29]

3.3. Crystallographic study

Suitable monocrystals of derivatives **11**, **13** and **14** were grown by slow evaporation of ethyl acetate solutions. Data were measured at 293 K on an Enraf–Nonius CAD4 diffractometer with graphite monochromated Cu Kα radiation. The structures were solved by direct method[21] and anisotropically refined by full matrix least-squares on *F* values.[22] Crystallographic data have been deposited with the Cambridge Crystallographic Data Centre as supplementary publication numbers CCDC 198528-198530. Copies of the data can be obtained, free of charge, on application to CCDC, 12 Union Road, Cambridge CB2 1EZ, UK [fax: +44-0-1223-336033 or e-mail: deposit@ccdc.cam.ac.uk].

Acknowledgements

The authors gratefully acknowledge the support of the Grant Agency of the Czech Republic (203/01/0634 and 203/03/0926).

References

1. (a) Hayashi, T.; Ogoshi, H. *Chem. Soc. Rev.* **1997**, *26*, 355–364. (b) Ward, M. D. *Chem. Soc. Rev.* **1997**, *26*, 365–375. (c) Anderson, H. L. *Chem. Commun.* **1999**, 2323–2330. (d) Patten, P. G. V.; Shreve, A. P.; Lindsey, J. S.; Donohoe, R. J. *J. Phys. Chem. B* **1998**, *102*, 4209–4216.
2. Sanders, J. K. M. *The Porphyrin Handbook*; Kadish, K. M., Smith, K. M., Guilard, R., Eds.; Academic: New York, 2000; Vol. 3, pp 347–368.
3. For books on calixarenes see: (a). In *Calixarenes*; Asfari, Z., Böhmer, V., Harrowfield, J., Vicens, J., Eds.; Kluwer Academic: Dordrecht, 2001. (b) Gutsche, C. D. In *Calixarenes revisited. Monographs in Supramolecular Chemistry*; Stoddart, J. F., Ed.; The Royal Society of Chemistry: Cambridge, 1998; Vol. 6. (c) In *Calixarenes 50th Aniversary: Commemorative Issue*; Vicens, J., Asfari, Z., Harrowfield, J. M., Eds.; Kluwer Academic: Dordrecht, 1994. (d) In *Calixarenes: A Versatile Class of Macrocyclic Compounds*; Vicens, J., Böhmer, V., Eds.; Kluwer Academic: Dordrecht, 1991.
4. Lhoták, P.; Shinkai, S. *J. Synth. Org. Chem., Jpn* **1995**, *53*, 963–974.
5. (a) Kumagai, H.; Hasegawa, M.; Miyanari, S.; Sugawa, Y.; Sato, Y.; Hori, T.; Ueda, S.; Kamiyama, H.; Miyano, S. *Tetrahedron Lett.* **1997**, *38*, 3971–3972. (b) Iki, N.; Kabuto, C.; Fukushima, T.; Kumagai, H.; Takeya, H.; Miyanari, S.; Miyashi, T.; Miyano, S. *Tetrahedron* **2000**, *56*, 1437–1443.
6. Dudic, M.; Lhoták, P.; Stibor, I.; Dvoráková, H.; Lang, K. *Tetrahedron* **2002**, *58*, 5475–5482.
7. (a) Gouterman, M. *The Porphyrins*; Dolphin, D., Ed.; Academic: New York, 1978; Vol. III, pp 1–165. (b) Nappa, N.; Valentine, J. S. *J. Am. Chem. Soc.* **1978**, *100*, 5075–5080.
8. (a) Chang, C. J.; Deng, Y.; Heyduk, A. F.; Chang, C. K.; Nocera, D. G. *Inorg. Chem.* **2000**, *39*, 959–966. (b) Fletcher, J. T.; Therien, M. J. *J. Am. Chem. Soc.* **2002**, *124*, 4298–4311.
9. Nagata, T.; Osuka, A.; Maruyama, K. *J. Am. Chem. Soc.* **1990**, *112*, 3054–3059.
10. Taylor, P. N.; Anderson, H. L. *J. Am. Chem. Soc.* **1999**, *121*, 11538–11545.
11. Kasha, M.; Rawls, H. R.; El-Bayoumi, M. A. *Pure Appl. Chem.* **1965**, *11*, 371–392.
12. Hunter, C. A.; Meah, M. N.; Sanders, J. K. M. *J. Am. Chem. Soc.* **1990**, *112*, 5773–5780.
13. Lhoták, P.; Šťastný, V.; Zlatušková, P.; Stibor, I.; Michlová, V.; Tkadlecová, M.; Havlíček, J.; Sýkora, J. *Collect. Czech. Chem. Commun.* **2000**, *65*, 757–771.
14. (a) Lhoták, P.; Himl, M.; Pakhomova, S.; Stibor, I. *Tetrahedron Lett.* **1998**, *39*, 8915–8918. (b) Lhoták, P.; Kaplánek, L.; Stibor, I.; Lang, J.; Dvořáková, H.; Hrabal, R.; Sýkora, J. *Tetrahedron Lett.* **2000**, *41*, 9339–9344.
15. (a) Lang, J.; Dvořáková, H.; Bartošová, I.; Lhoták, P.; Stibor, I.; Hrabal, R. *Tetrahedron Lett.* **1999**, *40*, 373–376. (b) Lang, J.; Vlach, J.; Dvořáková, H.; Lhoták, P.; Himl, M.; Hrabal, R.; Stibor, I. *J. Chem. Soc., Perkin Trans. 2* **2001**, *4*, 576–580.
16. Lhoták, P.; Dudič, M.; Stibor, I.; Petříčková, H.; Sýkora, J.; Hodačová, J. *J. Chem. Soc., Chem. Commun.* **2001**, 731–732.
17. X-Ray data for **11**: $C_{36}H_{70}O_8$, *M*=630.994, monoclinic

system, space group $P2_1/c$, a=10.171 (1), b=10.973 (1), c=27.928 (1) Å, β=97.58 (1)°, V=3089.7 (4) Å^3, Z=4, D_c=1.3564 g cm^{-3}, μ(Cu Kα)=7.398 cm^{-1}, crystal dimensions of 0.15×0.20×0.20 mm. Refined to final R=0.1001, R_w=0.0890 and S=1.0779 with 397 parameters using 3042 independent reflections (θ_{range}=3.19–67.90°). Hydrogen atoms linked to carbon atoms were located from expected geometry and were not refined. Hydroxyl hydrogen atoms were located from Fourier difference electron density map.

18. Very recently, similar data for the corresponding dimethyl- and diethylesters were published: Coles, S. J.; Hall, C. W.; Hursthouse, M. B. *Acta Crystalogr., Sect. C: Cryst. Struct. Commun.* **2002**, *C58*, o29–o31.
19. X-Ray data for **13**: $C_{32}H_{28}O_8S_4$, M=668.808, triclinic system, space group $P-1$, a=9.498 (3), b=10.541 (3), c=16.023 (3) Å, α=99.06 (2), β=100.98 (2), γ=92.58 (2)°, V=1550.5 (7) Å^3, Z=2, D_c=1.4325 g cm^{-3}, μ(Cu Kα)=32.541 cm^{-1}, crystal dimensions of 0.3×0.3×0.6 mm. Refined to final R=0.0695, R_w=0.0618 and S=1.0506 with 401 parameters using 2150 independent reflections (θ_{range}=2.85–59.91°). Hydrogen atoms linked to carbon atoms were located from expected geometry and were not refined. Hydroxyl hydrogen atoms were located from Fourier difference electron density map. Ψ-scan was used for absorption correction.
20. X-Ray data for **14**: $C_{48}H_{60}O_8S_4$, M=893.237, triclinic system, space group $P-1$, a=12.466 (2), b=13.997 (2), c=16.778 (2) Å, α=82.55 (1), β=73.61 (1), γ=65.51 (1)°, V=2555.6 (7) Å^3, Z=2, D_c=1.1608 g cm^{-3}, μ(Cu Kα)=20.869 cm^{-1}, crystal dimensions of 0.2×0.3×0.5 mm. Refined to final R=0.0863, R_w=0.0759 and S=1.0942 with 541 parameters using 7226 independent reflections (θ_{range}=2.75–67.93°). Hydrogen atoms linked to carbon atoms were located from expected geometry and were not refined. Hydroxyl hydrogen atoms were located from Fourier difference electron density map. Ψ-scan was used for absorption correction.
21. Altomare, A.; Cascarano, G.; Giacovazzo, G.; Guagliardi, A.; Burla, M. C.; Polidori, G.; Camalli, M. SIR92-a program for automatic solution of crystal structures by direct methods. *J. Appl. Crystallogr.* **1994**, *27*, 435–435.
22. Watkin, D. J.; Prout, C. K.; Carruthers, J. R.; Betteridge, P. W.; Cooper, R. I. *CRYSTALS*; Chemical Crystallography Laboratory: Oxford, UK, 2001; Issue 11.
23. Brettar, J.; Gisselbrecht, J. P.; Gross, M.; Solladié, N. *Chem. Commun.* **2001**, 733–734.
24. Kubo, Y.; Ikeda, M.; Sugasaki, A.; Takeuchi, M.; Shinkai, S. *Tetrahedron Lett.* **2001**, *42*, 7435–7438.
25. Böhmer, W.; Jung, K.; Schön, M.; Wolff, A. *J. Org. Chem.* **1992**, *57*, 790–792.
26. Rudkevich, D. M.; Verboom, W.; Reinhoudt, D. N. *J. Org. Chem.* **1994**, *59*, 3683–3686.
27. Collins, E. M.; McKervey, M. A.; Madigan, E.; Moran, M. B.; Owens, M.; Fergusson, G.; Harris, S. J. *J. Chem. Soc. Perkin Trans. 1* **1991**, 3137–3142.
28. Iki, N.; Morohashi, N.; Narumi, F.; Fujimoto, T.; Suzuki, T.; Miyano, S. *Tetrahedron Lett.* **1999**, *40*, 7337–7342.
29. Connors, K. A. *Binding Constants, The Measurement of Molecular Complex Stability*; Wiley: New York, 1987.